RESEARCH ARTICLE

# Snake Lower Jaw Skin: Extension and Recovery of a Hyperextensible Keratinized Integument

JOURNAL OF EXPERIMENTAL ZOOLOGY
PART A
ECOLOGICAL GENETICS AND PHYSIOLOGY
A Journal of Integrative Biology

MATTHEW CLOSE[1,2]* AND DAVID CUNDALL[1]
[1]Department of Biological Sciences, Lehigh University, Williams Annex, Bethlehem, Pennsylvania
[2]Biology Department, Radford University, Radford, Virginia

## ABSTRACT

The skin of squamates consists of a keratinized epidermis divided into thick scale and thinner, folded interscale regions underlain by a dermis containing a complex array of fibrous connective tissues. We examined the skin of the lower jaw of watersnakes (*Nerodia sipedon*) to determine how skin morphology changes when highly stretched during ingestion of large prey. Video records of skin behavior in the lower jaws of watersnakes feeding on fish or anesthetized watersnakes being stretched on an Instron machine showed that most skin extension involves the interscale skin. The largest intermandibular separation recorded during feeding was 7.7× resting distance, but intermandibular separation reached 10× without tissue failure during mechanical testing. Histological and anatomical analyses of lower jaws fixed in resting, moderately or highly stretched conditions showed that stretching had little effect on scale regions of the epidermis. However, stretching flattened folds of interscale regions at both gross and cellular levels and imposed changes in epidermal cell shape. Stretching of the dermis is primarily limited to realignment of collagen and stretching of elastin in the deep dermis. The configuration of dermal elastin suggests a model for passive recovery of epidermal folding following release of tension. *J. Exp. Zool. 321A:78–97, 2014.* © 2013 Wiley Periodicals, Inc.

*J. Exp. Zool. 321A:78–97, 2014*

**How to cite this article: Close M, Cundall D. 2014. Snake lower jaw skin: Extension and recovery of a hyperextensible keratinized integument. J. Exp. Zool. 321A:78–97.**

The integument forms the outermost layer of all metazoan bodies, and its form and function vary considerably (Brusca and Brusca, 2003; Kardong, 2012). In jawed vertebrates, it covers the ventral surface of the jaw apparatus and must accommodate changes induced when the mouth is opened during feeding. In snakes, the mandibular symphysis is highly modified or absent, one of a series of anatomical changes that allows them to swallow large prey whole (Gans, '61; Young, '98a,b; Kley, 2006). The soft tissues linking the mandibles determine how far the mandibles can separate, and this distance partly determines overall gape size (Arnold, '83; Cundall and Greene, 2000). It has been illustrated previously that in order for the mandible tips to separate, the skin covering the lower jaw and suspensorium must be extensible and/or connected loosely to the mandibles (Gans, '74). However, the mechanism of skin extension and recovery and the morphological diversity of skin and its attachment to the mandibles have yet to be determined.

The basic morphology of squamate skin was described previously by Ficalbi (1888), Lange ('31), Pockrandt ('37), and Maderson ('64). To summarize, the epidermis of snakes consists of scale and interscale regions (*hinge* of Maderson ('64) and Mittal and Singh ('87b), *inner scale surface + hinge* of Alibardi and

Grant sponsor: E.E. Williams Graduate Research Grant; grant sponsor: Herpetologists' League.
Conflicts of interest: None.
*Correspondence to: Matthew Close, Biology Department, Radford University, Box 6931, Radford, VA 24142-6939.
E-mail: mclose2@radford.edu
Received 4 February 2013; Revised 15 July 2013; Accepted 13 September 2013
DOI: 10.1002/jez.1839
Published online 8 November 2013 in Wiley Online Library (wileyonlinelibrary.com).

Thompson ('99), or *intersquamous* of Savitzky et al. (2004) and Rivera et al. (2005)) that are continuous. Both regions consist of a stratum germinativum composed of cuboidal (interscale) or columnar (scale) cells on which rest one to several layers of differentiated cells. These superficial layers of the interscale region also contain some presumptively undifferentiated (Mittal and Singh, '87b) living cells (*cellules à mamelon* of Ficalbi, 1888). As in other vertebrates, the cells of the stratum germinativum are anchored to the basement membrane at their basal surfaces via hemidesmosomes (Roth and Jones, '67) and to neighboring cells at their lateral and apical surfaces via desmosomes (Roth and Jones, '67). The superficial layers of scales consist of an α-layer (α-keratin, Baden et al., '66), a mesos layer, a β-layer (β-keratin, Baden et al., '66), and finally a thin superficial Oberhäutchen, and these layers have received most of the attention in the literature within the contexts of development (Maderson, '65b; Maderson, '85; Alibardi, 2002; Alibardi and Thompson, 2003; Swadźba and Rupik, 2010a,b), the shedding cycle (Maderson, '65b; Roth and Jones, '67, '70; Mittal and Singh, '87a,b) and micro-ornamental specializations in scale Oberhäutchen (Price, '81, '82; Irish et al., '88; Chiasson and Lowe, '89; Chiasson et al., '89; Gower, 2003; Joseph et al., 2007). The scales also house the major epidermal sense organs of the skin (Jackson and Sharawy, '80).

The interscale region was described by Ficalbi (1888), Pockrandt ('37), and Maderson ('64) but has received relatively little attention in the literature since. It was the primary subject of a single study on the shedding cycle (Mittal and Singh, '87b), but is noted briefly in most studies of the shedding cycle (Maderson, '65a; Roth and Jones, '67, '70; Banerjee and Mittal, '80) or skin development (Alibardi, 2002; Alibardi and Thompson, 2003; Swadźba et al., 2009; Swadźba and Rupik, 2010a,b). To summarize the findings of studies mentioned above, the interscale epidermis of squamates is thrown into folds that are thought to serve a variety of functions (Maderson, '64; Roth and Jones, '67; Jackson and Reno, '75; Lillywhite and Maderson, '82; Sherbrooke and Scardino, 2007). The interscale epidermis shares most layers with the scale region but lacks the thickened β-layer (and thus most of the hard β-keratins that give the scale region its stiffness), and the mesos and α-layers are thin and difficult to distinguish. The Oberhäutchen is thin and the surface is characteristically bumpy. The keratins of the interscale region are predominantly α-keratins, and it is thought that the region should differ from the scale region in its mechanical properties and secretory capabilities (Banerjee and Mittal, '78, '80; Mittal and Singh, '87a,b; Alibardi and Thompson, '99). Therefore, if the epidermis of snakes is an extensible stratified squamous epithelium, then understanding the structure and function of the interscale regions is critical to understanding skin's mechanical behavior.

Reviews and discussions of the structure and function of the vertebrate dermis have illustrated the importance of the organization and composition of its collagen and elastin fibers to the mechanical behavior of the whole integument (Montagna, '62; Montagna et al., '70; Moss, '72; Landmann, '86). Despite this, and the apparent accepted phenomenon of skin extensibility in snakes, descriptions and discussion of the dermis in snakes are scarce. Pockrandt ('37), Roth and Jones ('67), and Jackson and Reno ('75) recognized both dermal and epidermal components to snake scales, pointing out that the dermis is thickest near the center of the scale and thinnest near the lateral and caudal free margins. Maderson ('65b) and Alibardi (2002) described the development of the dermis in the outer and inner [marginal] scale surfaces and hinge regions of lizards and snakes, but unfortunately provided few details on the interscale region alone. From these studies, it is clear that the dermis of the scale region consists of at least two layers: a thick, superficial *stratum laxum* of loosely organized collagen and uniformly distributed mesenchymal fibroblasts and a deep *stratum compactum* composed of dense, parallel-fibered collagen and flattened, randomly distributed fibroblasts. Licht and Bennet ('72), in their study of a scaleless *Pituophis melanoleucus catenifer*, showed that the superficial dermis was entirely absent in scaleless specimens and that this component was the "major morphological element" of the scale. Alibardi (2002) also recognized a third layer of "loose" subdermal reticular fibers that are apparently orthogonal to the axis of the scale (see Fig. 9 from Alibardi, 2002). The latter suggests that the dermis of late-stage snake embryos possesses a structurally and functionally divided dermis, though the structure is not well described and the functions are speculative.

If we assume that the dermis of snakes is similar to that of other vertebrates in its structure and composition, it should be composed of collagen, elastin, fibroblasts, and ground substance. Although the aforementioned studies showed that the dermis is structurally divided (i.e., scale regions are composed of both a superficial layer of loose, orthogonally arranged collagen fibers and a deep layer of dense, parallel collagen fibers while interscale regions are dominated by dense, parallel collagen fibers) only Pockrandt ('37) distinguished both collagen and elastin in the two regions and ascribed hypothetical mechanical functions to each region. To date, two published studies on the tensile properties of snake skin (Jayne, '88; Rivera et al., 2005) and one unpublished account (Savitzky et al., 2004) have placed the dermis as a key structural element to snake skin extensibility and have attempted to relate dermal organization to the skin's behavior. However, no study has indentified which parts of the snake integument define the limits to its extensibility and none has provided a mechanism for passive recovery from highly extended states. The biomechanical properties of collagen have been well studied in most connective tissues, and collagen likely accounts for much of the skin's ability to resist mechanical failure (Fratzl, 2008). In mammalian skin, at low levels of strain (up to about 20%) there is little change in the tissue's mechanical properties because collagen, which is organized in orthogonal cross-plies, undergoes reorientation prior to stretching and slippage. At increased loads the latter account for skin's viscoelastic properties. However, under prolonged periods

of strain, collagen alone is incapable of full recovery from high levels of extension due to irreversible creep. Montagna ('62) and Partridge ('70) suggested previously that elastin in the deep dermis should be responsible for skin's elastic behavior, but this has not been supported by in vivo or in vitro studies of mammalian skin. Given the established structure and function of elastin (Partridge, '70; Oxlund et al., '88; Debelle and Tamburro, '99), it is likely (as was suggested by Savitzky et al., 2004 and Rivera et al., 2005) that elastin in the dermis of snakes is responsible for the refolding of interscale skin and subsequently for returning the skin to its resting condition after prolonged periods of stretch.

The skin and intermandibular soft tissues determine the lower jaw's extensibility and the upper jaws of snakes are limited in the degree to which they can move laterally. Therefore, suspensorial length and mobility, mandible length and lower jaw extensibility are the major determinants of gape size in snakes (Arnold, '83; Cundall and Greene, 2000). Within the context of macrostomy, we examined how skin behaves during swallowing and then related function to structure. We first asked how scale and interscale regions of lower jaw skin respond to stretch during swallowing events at the gross level. Based on previous descriptions of skin morphology, which showed distinct structural differences between the scale and interscale epidermis and dermis, we expected scale and interscale regions to respond to stretch differently. Specifically, we predicted that during swallowing events, the width of lower jaw scales would not increase when the lower jaw is extended during maximum gape, whereas the distance between adjacent scales would increase. Secondly, we asked how our behavioral results related to gross and microanatomy by both qualitatively and quantitatively describing the changes that occur between resting, moderately stretched and highly stretched lower jaws. Specifically, we expected low to moderate levels of extension to impose unfolding of the interscale regions, but we expected moderate to high levels of extension to stretch this region. Therefore, we predicted that although gross anatomical effects would be seen at levels of moderate stretch, major histological and cytological changes associated with stretching (primarily deformation of tissues and cells) would be most evident at higher levels of extension. Finally, we asked which epidermal and/or dermal features define the structural limits to interscale skin extensibility and sought to provide a model for the skin's passive recovery following stretch.

## METHODS

### Animals

Northern watersnakes (*Nerodia sipedon sipedon*) were collected locally, housed in the laboratory on a 12:12-hr light/dark cycle at 25–28°C, and given access to water ad libitum. Neonates born in the lab were reared under the same conditions. Adult snakes were fed shiner minnows (*Notemigonus crysoleucas*) and trout (*Oncorhynchus mykiss*, *Salmo trutta*, and *Salvelinus fontinalis*) every 7–10 days and neonates were fed fathead minnows (*Pimephales promelas*) every 4–7 days during the study.

### Feeding Behavior

Prior to feeding trials, snakes and prey were weighed and mass ratios (calculated as prey mass/snake mass) were obtained. Maximum height and width of the fish were measured, and these values were used to calculate prey cross-sectional area (calculated as the area of an ellipse using the equation: [$\pi \times$ height $\times$ width]/4). Prey cross-sectional areas ($CSA_{Prey}$) were combined with estimated cross-sectional areas of gape ($CSA_{Snake}$) derived from snake jaw lengths ([$\pi \times JL^2$]/4, JL measured as the distance from the anterior border of the mental scale to the caudal edge of the bulge formed by the retroarticular process of the mandible) in order to calculate ingestion ratios (calculated as $CSA_{Prey}$/$CSA_{Snake}$).

Neonates were fed in an arena that consisted of a glass plate floor with a mirror angled at 45° below, allowing for simultaneous lateral and ventral views of snakes during feeding (Fig. 1). Larger adults were fed in a larger feeding arena used previously by Cundall and Deufel (2006), allowing for similar views of larger specimens. All behavioral records were collected using either a Panasonic AG-456 VHS recorder (Panasonic Corporation, Kadoma, Osaka, Japan) or Cannon ZR900 miniDV camcorder (Cannon Inc., Ohta-ku, Tokyo, Japan). VHS records were analyzed by playing back tapes on a TV monitor and measuring distances directly on the monitor with a ruler. All miniDV records were captured and edited using FinalCut Pro software (Apple Computer, Inc., Cupertino, CA, USA). Still frames were analyzed using Image J software (National Institutes of Health, Bethesda, MD, USA).

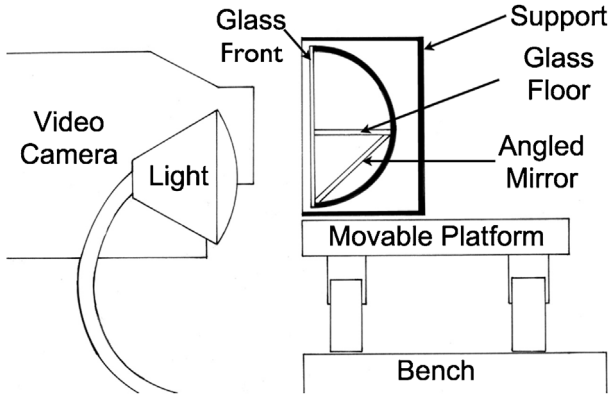


Figure 1. Diagrammatic view from the right end of the feeding arena used for neonate watersnakes. The arena was made of a 14 in. length of 1.5 in. PVC pipe cut in half and supported by wooden blocks. The mirror and glass pieces were fit into grooves cut in the wooden support panels. The entire arena sat on a rolling dolly positioned immediately in front of the video camera and light source.

Table 1. Summary of behavioral records for *Nerodia sipdeon*.

| Individual | # Trials | Mass ratio (%) | $CSA_{Prey}/Gape_{Estimated}$ |
|---|---|---|---|
| Adult 1 | 1 | 30 | 62 |
| Adult 2 | 5 | 35–84[a] | 75–107[a] |
| Adult 3 | 1 | 46 | 45 |
| Adult 4 | 3 | 32–90[a] | 52–109[a] |
| **Neonate 1** | 4 | 30–44 | 41–60 |
| **Neonate 2** | 5 | 30–59 | 46–63 |
| Neonate 3 | 4 | 32–40 | 40–50 |
| Neonate 4 | 1 | 37 | 45 |
| **Neonate 5** | 1 | 39 | 59 |
| **Neonate 6** | 6 | 30–45 | 37–92 |
| **Neonate 7** | 5 | 34–53 | 36–63 |
| Neonate 8 | 6 | 32–58 | 27–78 |
| Neonate 9 | 5 | 31–57 | 39–70 |
| **Neonate 10** | 1 | 31 | 38 |
| Neonate 11 | 1 | 45 | 41 |
| ***n* = 15** | ***n* = 49** | **30–90[a]** | **27–109[a]** |

Individuals in bold are those later used for anatomical and/or histological analyses. Values for ratios are ranges.
[a]Denotes an event in which an attempt was made by the snake to ingest prey, but regurgitated after maximum gape had been achieved.

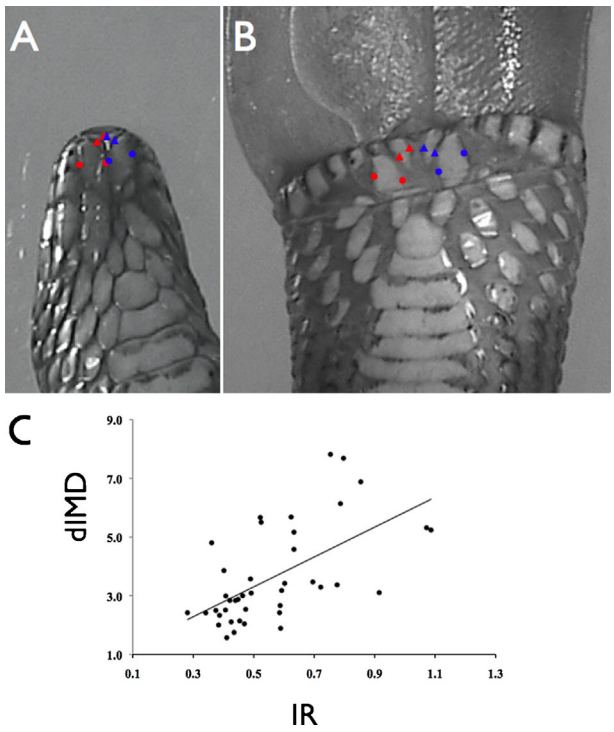


Figure 2. (A, B) Still frames captured from video of a Northern watersnake swallowing a trout 40% its body mass. (A) Ventral view of head at rest. Markers indicate the borders of the right and left first lower labials (▲) and anterior chin shields (●). (B) Ventral view of head at maximum gape, with markers as in (A). The width of scales increases slightly and significantly upon stretch, but the increase is significantly smaller than the increase in distance between scales. (C) Plot of ingestion ratio (*x*) on change in intermandibular distance (*y*) during feeding trials.

Video records of feeding (Table 1) were analyzed for dynamic changes in skin during feeding trials. In lieu of marking animals prior to feeding trials, digital markers were placed at points along the medial and lateral margins of first lower labials ($L1_R$, $L1_L$) and anterior chin shields ($A_R$, $A_L$) from still video frames (Figs. 2A, 2B). For the first lower labials we placed a point directly anterior to a distinct 135° bend in the medial margin, and then placed a second point on the lateral margin at the end of a line that originated at our first point and was orthogonal to the lateral margin of the scale. For digitally marking the anterior chin shield, we first placed a point on its medial margin directly behind the overlapping posterior free margin of the first lower labial. We then placed a second point on the lateral margin at the end of a line drawn from the first point orthogonal to the lateral margin. This region was chosen because, from a superficial view, it was the only region where data on two-scale relationships can be accurately obtained and where interscale distances could be measured easily in vivo without marking scales prior to the feeding trial. All other scales of the lower jaw overlap, and thus the lateral margins of adjacent scales are impossible to see in the resting condition.

The distance between markers was measured at rest either prior to or immediately following a swallowing sequence and at the largest gape recorded. The latter occurred when both gape angle (measured as the angle formed between the braincase and the lower jaw axes) and intermandibular distance (measured as the distance between the tips of the mandibles) were at their highest values. Univariate linear regression was used to scale change in intermandibular distance to ingestion ratios (Fig. 2C). All values measured from video records were scaled to known distances from the feeding arena. To correct for differences in size between individuals, values were scaled to lower jaw length.

Changes in distance between markers were compared between scale and interscale regions, and data were analyzed using a two-way ANOVA, testing for interactions between treatment group (resting vs. stretched) and skin region (scale vs. interscale).

### Mechanical Testing

Uniaxial tensile tests were carried out on two adult watersnakes in order to determine the loads attained when the mandibles were extended under conditions similar to those seen during feeding trials. To do this, snakes were anesthetized with 30 mg/kg of pentobarbital and their mandibles were secured in clamps designed by DC that gripped the mandibles while allowing the skin and soft tissues lateral to the mandibles to roll through the clamp as strain increased. The clamps were fixed in an Instron

5567 tensile testing machine fitted with a 500N load cell (Instron, Norwood, MA, USA).

Extension limits were initially set at 7× resting snake intermandibular distance, and extension was applied at a ramp rate of 0.0167 mm/s. To simulate swallowing-like behavior for our mechanical tests, we programmed periods of rest that started with 30 sec and gradually increased to 300 sec as extension increased. Therefore, the total time for a mechanical test varied from 45 min to 1 hr depending on the individual tested. The interior of the mouth was irrigated with water during testing to prevent the mucosa from drying. Snakes recovered following the tests and regained normal feeding activities. A second trial was conducted on one individual after 4 months, and the extension limit was increased to 10× resting intermandibular distance.

### Mechanical Manipulations for Anatomical and Histological Preparations

Specimens were anesthetized with isoflurane, received one of three treatments, and were sacrificed by overdose with anesthesia or by decapitation following anesthesia. One group received no treatment and was fixed in the resting condition with 10% phosphate-buffered formalin. In this group, the mouth was opened slightly to allow the oral cavity and anterior gut to be flooded with fixative. Intermandibular distance was measured using either dial calipers or, for smaller snakes, an ocular micrometer or miniscale (Micro-Tool™ Agar Scientific, Elektron Technology UK Ltd., Stansted, Essex, UK).

For the stretch treatment groups, the right mandible was pinned to a dissecting tray using hooks fashioned from 00 or 0 insect pins, and the left mandible was gripped with forceps and extended laterally to approximately 2× its resting distance. The left mandible was then pinned and allowed to rest for a period of five minutes. It was then unpinned and subsequently extended to 3× resting distance. For moderately stretched specimens, the lower jaws were fixed between 3 and 5× resting distance. For highly stretched specimens, the process of rest and extension was repeated over periods of 20 min to 1 hr until the mandibles were between 5 and 7× resting distance. This was done to simulate normal physiological conditions, ensuring that the mandibles were extended to ranges seen in behavioral records of snakes feeding on the largest prey taken and to allow time for the soft tissues to adapt to the strain. Each animal was then fixed in the stretched condition with 10% phosphate-buffered formalin.

### Anatomy

Lower jaws were removed from fixed specimens and stored in 70% ethanol. In order to obtain detailed anatomical information on lower jaws prior to further processing, specimens were drawn, photographed, and/or measured using either an ocular micrometer or a miniscale. The following measurements of scales (Fig. 3) were collected in order to compare resting with stretched specimens: DMG, distance between mental and first labial scales; DGG, distance between first labial scales; DGA, distance between first lower labials and anterior chin shields; DAA, distance between anterior chin shields; DAL2,3,4, distance between anterior chin shields and infralabials 2, 3, and 4; DPP, distance between posterior chin shields; DPL4,5,6, distance between posterior chin shields and infralabials 4, 5, and 6. Scales were measured from the approximate center of each scale, defined as a point midway between anterior and posterior borders and lateral and medial margins.

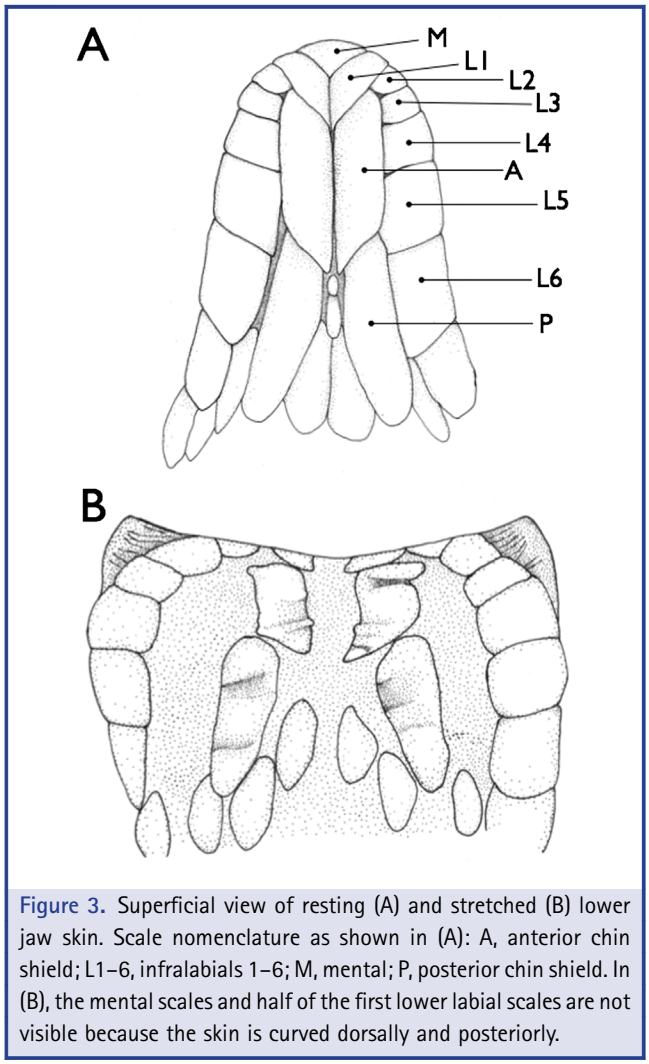


Figure 3. Superficial view of resting (A) and stretched (B) lower jaw skin. Scale nomenclature as shown in (A): A, anterior chin shield; L1–6, infralabials 1–6; M, mental; P, posterior chin shield. In (B), the mental scales and half of the first lower labial scales are not visible because the skin is curved dorsally and posteriorly.

Resting, moderately stretched and highly stretched specimens were used for microdissection (Table 2). The skin was removed carefully from the level of the jaw joint, working rostrally towards the first lower labial scale. Complete removal of the skin could not be accomplished without removing important intermandibular connective tissues, and the skin was reflected at the most anterior point possible (without destroying these tissues) at the anterior edge of the mental scale. Removal of the skin required severing of several

Table 2. Summary of anatomical and histological samples examined.

| | Treatment group | | |
|---|---|---|---|
| Sample type | Resting | Moderately stretched | Highly stretched |
| Anatomical | Neonate 12 | Adult 4 | |
| | **Neonate 1**[CS] | **Neonate 2** | Neonate 16[SEM] |
| | Neonate 13 | **Neonate 5** | Neonate 17[a] |
| | Neonate 14[SEM] | **Neonate 10** | Neonate 18[CS] |
| | **Neonate 7** | Adult 6 | **Neonate 6** |
| | Neonate 15[CS] | | Adult 7 |
| | Adult 5[SEM] | | Adult 8[SEM] |
| ***n*** **= 18** | *n* = 7 | *n* = 5 | *n* = 6 |
| Histological | Neonate 19 | Neonate 25 | Neonate 28 |
| | Neonate 20 | Neonate 26 | Neonate 29 |
| | Neonate 21 | Neonate 27 | |
| | Neonate 22 | | |
| | Neonate 23 | | |
| | Neonate 24 | | |
| ***n*** **= 11** | *n* = 6 | *n* = 3 | *n* = 2 |

CS, specimens that were cleared and stained; SEM, specimens prepared for scanning electron microscopy.
[a]Specimen that was stretched to the point of failure.

distal branches of the trigeminal nerve innervating the scales. Therefore, intact networks of major nerves innervating the scales were later identified using a small sample of cleared and stained specimens (Table 2; Nishikawa, '87). Once identified, we were able to compare intact networks with severed branches attached to the dorsal surface of the skin and better identify neurovascular bundles and their attachments to the skin. These were then mapped and compared for both resting and stretched specimens.

### Histology

Resting, moderately stretched and highly stretched specimens (neonates and juveniles) were prepared for light microscopy (Table 2). Samples were dehydrated through a series of graded ethanols, cleared in xylene, and embedded in paraffin. Blocks were sectioned at 5–10 μm, and sections were mounted into three series. Each series was stained with H&E, iron gallein elastin stain (Churukian and Schenk, '76), or Masson Trichrome (Humason, '79) for connective tissues. Resting and stretched specimens were then examined using a Nikon Eclipse 50i compound light microscope (Nikon Corporation, Tokyo, Japan) fitted with a Nikon Digital Sight DS-5M CCD camera (Nikon Corporation). All measurements were made using a Nikon Digital Sight DS-L2 control unit (Nikon Corporation).

In order to determine the histological effects of stretching, scale and interscale regions were compared at two locations from anterior snake lower jaws. The first region consisted of the area between and including anterior chin shields and the second comprised the region between and including the anterior chin shield and adjacent labial scales. Effects of stretching on the superficial epidermis were difficult to determine because the keratinized layers tended to be at least partially removed either during dehydration or during sectioning. In addition, because time since shedding had not been established prior to sample preparation it was difficult to assess how and whether the shedding complex influenced stretch treatment.

Effects of stretching on the epidermis were quantified using the following set of variables: (1) Fold amplitude (FA) was measured as the amplitude of the major folds of interscale skin. FA was only measured for interscale skin because folds do not appear in the scale regions. A minimum of three folds was measured from both sample areas in each section, and a total of five sections containing each region of interest was analyzed and averaged. Therefore, 60 samples from each area were averaged for resting and stretched treatment groups. (2) Internuclear spacing of stratum germinativum cells, EINS (Fig. 4), was measured as the linear distance between a pair of adjacent nuclei of the stratum germinativum. A total of 10 pairs of nuclei were sampled for scale and interscale regions in each section, and 5 sections were averaged from 4 specimens each, to yield a total of 200 points for scale and interscale regions of each area sampled in unstretched and stretched treatment groups.

Since the vertebrate dermis is a composite tissue containing primarily collagen, ground substance, elastin, and fibroblasts (Gibson and Kenedi, '70) and since the dermis is distinctly different

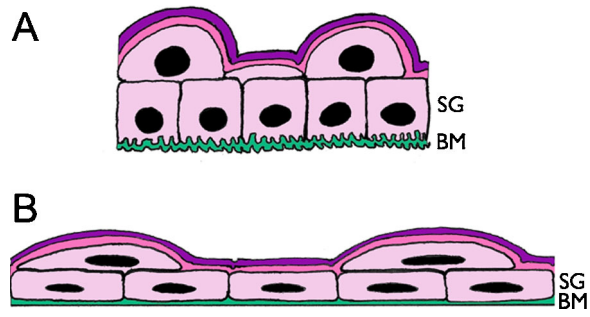


Figure 4. Internuclear spacing in the epidermis (EINS). (A) Resting condition. (B) Stretched condition. In the resting condition, the basement membrane (BM) and adjacent cell membranes are convoluted. Cells of the stratum germinativum (SG) are anchored to the basal lamina of the BM via hemidesmosomes, and are anchored to adjacent cells via desmosomes. When the epithelium is stretched, the BM unfolds and the cells lengthen in the direction in which load is applied. This causes a decrease in the cross-sectional area of cells and an increase in the distance between nuclei of adjacent cells, which serves as a relative indication of the strain of the epithelium.

in composition along its depth, we first determined its relative elastin composition using differential point counting of serial sections. To accomplish this, serial sections of dermis were selected and a digital 100-square grid was overlain on the image in the microscope's control unit. Each cell of the grid was then scored as being primarily composed of elastin if elastin made up more than 50% of the total area of relative composition along the depth of the dermis, from superficial dermis to the deep dermis, in each region. We then compared scale and interscale regions of dermis for the two areas sampled.

Since, as in most vertebrates, collagen fiber distribution and orientation were distinctly different between superficial and deep dermis, we characterized fiber orientation/arrangement as being transverse/parallel, transverse/woven, or orthogonal, and noted orientation changes between resting and stretched specimens. Because the quantitative effects of stretch on collagen are difficult to determine with the light microscope, we quantified the effect of stretch on the dermis using dermal fibroblast internuclear spacing, DINS. Our use of measuring DINS was underlain by the assumption that as the extracellular matrix changes during mechanical events, fibroblasts will stretch relative to one another in the plane of extension. While cytoplasmic processes are not easily distinguished with the light microscope, the nuclei are relatively distinct and should give an approximation of how far fibroblasts stretch relative to one another during extension events (Fig. 5). DINS was measured for 10 pairs of fibroblast nuclei from the superficial and deep dermis of the scale region and the dermis of the interscale region for five sections from each region sampled.

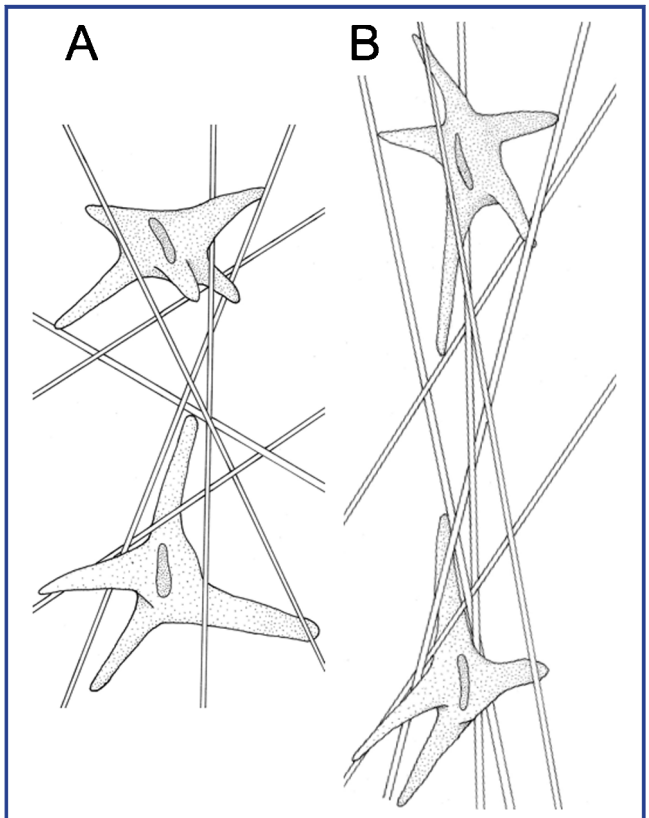


Figure 5. Dermal fibroblast internuclear spacing (DINS). (A) Resting condition. (B) Stretched condition. As the collagen fibrils in the extracellular matrix are reoriented, the fibroblasts migrate and/or are stretched in the direction in which the load is applied. The distance between adjacent fibroblast nuclei therefore gives a relative measure of strain of the extracellular matrix during a mechanical event.

### Scanning Electron Microscopy

A small sample of resting and stretched specimens was used to compare regional differences in response to stretch using scanning electron microscopy (Table 2). Skin was removed from the lower jaw and the medial margin of the right anterior chin shield was removed to expose the interscale epidermis. The left anterior chin shield's right margin remained intact. Samples were dehydrated through a series of graded ethanols, air dried, and mounted to stubs with conductive tape. All samples were then viewed with a Hitachi TM-1000 (Hitachi, Ltd., Chiyoda-ku, Tokyo, Japan) scanning electron microscope. From images collected using the computer's viewer program, we subsequently measured major and minor axes of 50 resting and 50 stretched *cellules à mamelon* (Ficalbi, 1888), a large, superficial, presumably undifferentiated cell (Mittal and Singh, '87b) of the interscale region, using Image J software.

All methods were approved under Lehigh University IACUC Protocol 66.

### Statistical Analyses

Differences in our set of scale–scale distances among treatment groups were tested using a one-way multivariate analysis of variance (MANOVA). Univariate, pairwise Fisher's LSD comparisons were then used to determine how individual pairs of scales differed under each treatment and which pairs were consistently different between treatments. Differences in each of our histological variables among treatment groups were tested using multiple one-way ANOVAs, and in cases where histological variables were shared between scale and interscale regions, we instead used two-way factorial ANOVAs to test for interactions between treatment and region. In all cases, pairwise Fisher's LSD comparisons were used to test for significant differences among groups. All statistical analyses were conducted using PASW Statistics 18 software package (IBM Corp., Armonk, NY, USA).

## RESULTS

### Feeding Behavior and Mechanical Testing

Relative prey sizes used in this study ranged from 30% to 90% for mass ratios and 27–109% for ingestion ratios (Table 1). Gape angle

ranged from 41° to 62°, intermandibular distance ranged from 2.5× to 7.7× resting distance, and time to reach maximum gape occurred between 8 and 20 min after swallowing began. These results provided the data used to establish both the parameters of mechanical testing as well as experimental manipulations used for determining skin function.

The maximum loads imposed on the intermandibular soft tissues in vivo was 1.9 N, occurring at 10× resting intermandibular distance (Figs. 6A, 6B). Introducing rest periods into the test increased the total time that the tissues were extended and allowed for time for the tissues to adapt between increases. Therefore, within each period of increase the load versus extension increased sharply, whereas the increase overall was slow and more linear (Fig. 6B). In none of the mechanical tests did the lower jaws reach failure, and both animals tested recovered fully. In combination with our behavioral measures, these results showed that the limit to lower jaw extensibility was (1) greater than in any of our feeding trials (10× resting IMD as compared to 7.7× resting IMD) and (2) a time-dependent process.

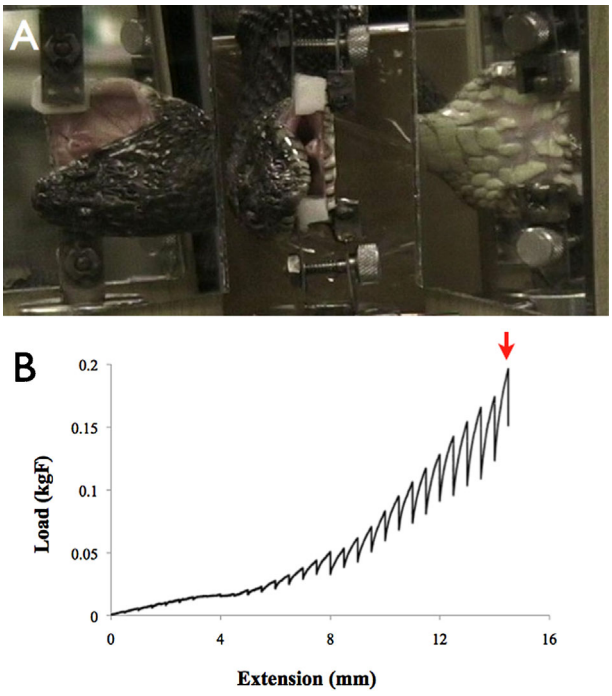


Figure 6. Mechanical testing of intermandibular soft tissues. (A) Dorsal (left), rostral (middle), and ventral (right) views of an adult watersnake in mechanical testing apparatus at maximum extension. (B) Plot of load versus extension data for the individual shown in (A). Arrow indicates point at which 10× intermandibular distance (measured from resting intermandibular distance) was achieved.

### General Description of the Gross- and Microanatomical Organization of Snake Epidermis

Superficially, the snake integument consisted of keratinous scales, and in the resting condition, scales typically overlapped or abutted one another. The borders of some scales were evident in the resting condition, but when the skin was extended, scale overlap was reduced dramatically and the edges of most of the scales as well as the softer interscale (*intersquamous*, *hinge*, or *hinge + inner scale surface* of others) skin lying between pairs of adjacent scales became evident (Fig. 3). While a distinction between scale and interscale regions was apparent at the gross level in the distended state, the histological organization of skin revealed key differences in organization that are important in permitting its extreme extensibility. Though the epidermis of scale and interscale regions consisted of a stratified squamous epithelium, the scale region (Fig. 7A) consisted of a distinct, thick superficial β-layer that was not developed in the interscale region. The interscale epidermis (Fig. 7A), on the other hand, consisted of a thin β-layer, barely visible with the light microscope. Furthermore, the interscale epidermis was characteristically bumpy and thrown into numerous folds, a condition not present in the scale. A scale's border was, therefore, defined by the point where the β-layer transitioned from thick and relatively smooth (scale) to thin, bumpy, and folded (interscale). This transition took place at or below the margins of the scales (Fig. 7A).

### Behavior of Skin In Vivo

In order to determine how skin regions (scale, interscale) responded differently to passive loads applied under normal physiological conditions, we compared the difference in distances within (scale width) and between (interscale distance) scales from two pairs of scales (first lower labials [L1], anterior chin shields [AC]) at resting and maximum achieved gape during swallowing events using two-way ANOVA. Data are provided in Table 3. Average scale width increased by 22% for first lower labials and 18% for anterior chin shields ($P < 0.05$), and interscale distance increased by 307% between first lower labials and 437% between anterior chin shields ($P < 0.05$). Interscale regions extended more than scale regions (interaction of treatment with region $P < 0.01$ for both scales), and increase in the width of scale regions occurred due to bending of the free margins of scales rather than lengthening of the structure (see below).

### Gross Anatomical Effects of Extension

We examined the effects of lower jaw extension on scale displacement by comparing specimens whose lower jaws had been manually stretched in vivo and subsequently fixed in *resting*, *moderately stretched*, or *highly stretched* positions. We compared distances between scales for 11 scale pairs across our three stretch treatment groups using one-way MANOVA. Data are shown in Table 4. Our analysis indicated that the three treatment groups differed significantly (Wilks' $\Lambda = 0.00$, $F = 19.68$, $P < 0.01$).

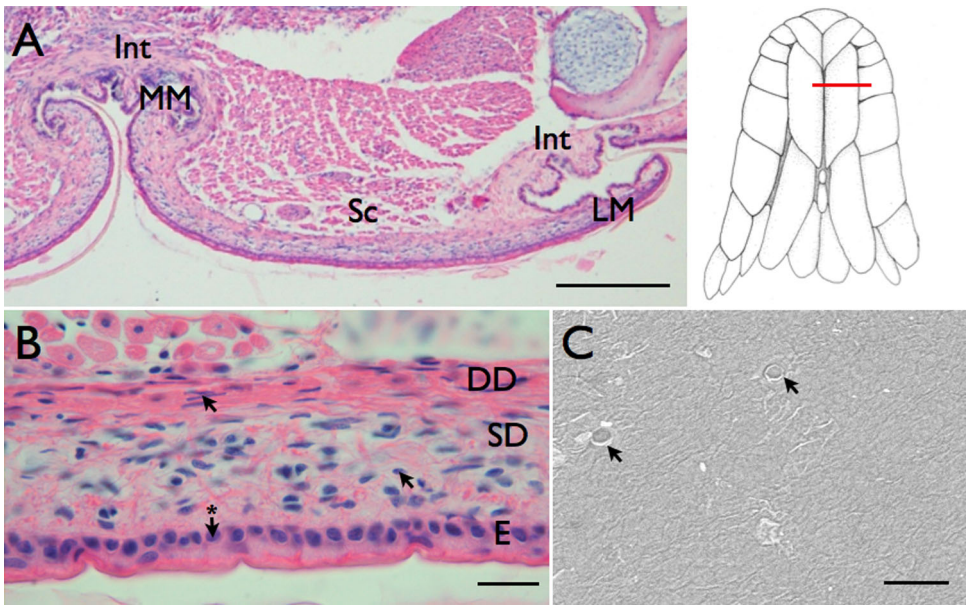


Figure 7. Cross-section of anterior chin shield at the level shown at insert on right. (A) H&E stain, scale bar = 100 μm. Scale (Sc) and interscale (Int) regions shown as well as lateral (LM) and medial (MM) scale margins. (B) Scale region, H&E stain, scale bar = 10 μm. Epidermis (E) is shown and the dermis is divided into superficial (SD) and deep (DD) regions. Arrows without * indicate location of fibroblast nuclei. Arrow with * indicates a nucleus of an epidermal stratum germinativum cell. (C) SEM image of outer scale surface, scale bar = 20 μm. Arrows indicate external pits in the Oberhäutchen associated with epidermal sense organs (tubercles).

However, post hoc comparisons of distances between scale pairs across treatments showed that displacements were not significant for all scales across the three treatments (Table 5). The absolute distances between several pairs of scales did not increase across all treatments due partly to three-dimensional relationships. Specifically, whereas scale–scale distances were measured between the centers of scales, the angle of scales relative to one another and to the plane of stretch was variable. In other words, although the lower jaw was stretched only in the circumferential direction, scales were displaced from their original positions in two dimensions. Interscale distance (i.e., the distance between scale margins, as measured in our behavioral analyses) may then increase without a significant net increase in distance between scale centers.

Scale pairs L1L1, AA, AL4, PP were the only pairs whose scale–scale distance consistently increased across all treatment groups (Table 5). Because the area between posterior chin shields contained additional scales fully or partially hidden in the resting condition, the pairs that provide the best data on single scale–scale relationships across treatment groups used in our study were L1L1, AA, and AL4. L1L1 and AA had scale margins that abut one another at the midline, but the scale margins of

Table 3. Average ± SD change in scale widths (SW) and interscale distances (INT) of first lower labials and anterior chin shields during swallowing events.

| | First lower labials | | Anterior chin shields | |
|---|---|---|---|---|
| | SW (mm) | INT (mm) | SW (mm) | INT (mm) |
| Min | 0.038 ± 0.010 | 0.0074 ± 0.0048 | 0.090 ± 0.016 | 0.012 ± 0.010 |
| Max | 0.047 ± 0.014 | 0.030 ± 0.017 | 0.11 ± 0.019 | 0.062 ± 0.029 |
| % Change | 24% | 305% | 22% | 416% |
| $F_{(1,78)}$ | 9.99 | 127.88 | 18.35 | 106.00 |
| $P$ | <0.01 | <0.01 | <0.01 | <0.01 |

Table 4. Superficial anatomical effects of lower jaw stretching on lower jaw scale spacing under resting (rest), moderately stretched (mod), and highly stretched (high) treatments.

| | Treatment | | |
|---|---|---|---|
| $Scale_1$–$scale_2$ | Rest ($n=8$) | Mod ($n=3$) | High ($n=6$) |
| M–L1 | 0.07 ± 0.008 | 0.08 ± 0.013 | 0.09 ± 0.011 |
| L1–L1 | 0.08 ± 0.013 | 0.10 ± 0.015 | 0.13 ± 0.019 |
| L1–A | 0.13 ± 0.031 | 0.11 ± 0.019 | 0.10 ± 0.017 |
| A–A | 0.10 ± 0.013 | 0.15 ± 0.023 | 0.19 ± 0.015 |
| A–L2 | 0.15 ± 0.032 | 0.12 ± 0.016 | 0.13 ± 0.022 |
| A–L3 | 0.13 ± 0.016 | 0.13 ± 0.016 | 0.15 ± 0.030 |
| A–L4 | 0.11 ± 0.018 | 0.16 ± 0.012 | 0.19 ± 0.032 |
| P–P | 0.13 ± 0.021 | 0.23 ± 0.031 | 0.32 ± 0.062 |
| P–L4 | 0.26 ± 0.014 | 0.23 ± 0.008 | 0.26 ± 0.026 |
| P–L5 | 0.18 ± 0.038 | 0.20 ± 0.036 | 0.24 ± 0.044 |
| P–L6 | 0.11 ± 0.170 | 0.21 ± 0.020 | 0.25 ± 0.067 |

Values are means ± SD of scale–scale distance scaled to jaw length in order to account for size differences among individuals.

AL4 overlapped, making accurate measures of interscale distance change impossible for this pair of scales.

### Histology: Epidermal Changes

The thickness of the epidermis proved to be difficult to measure across all treatment groups, and because all superficial keratinized layers were difficult to detect with the light microscope, thickness was not used to compare groups quantitatively. Furthermore, in the bumpy, folded regions of interscale epidermis, apparent thickness varied considerably. However, the stratum germinativum was distinguishable across all treatment groups and between scale and interscale regions, and therefore measures of epidermal internuclear spacing (EINS) provided data on the quantifiable changes accompanying extension across treatment groups.

We compared EINS across treatment groups and between scale and interscale regions in the area between the anterior chin shields (AA) using a two-way factorial ANOVA. When comparing treatments using averages of scale and interscale means, there was a significant increase in EINS across treatment groups ($F_{(2,746)} = 67.67$, $P < 0.01$). Specifically, compared to the resting condition, EINS was 15% higher ($P < 0.01$) in the moderately stretched condition and was 29% higher ($P < 0.01$) in the highly stretched condition. Furthermore, EINS was 12% higher in the highly stretched condition than in the moderately stretched condition ($P < 0.01$). A significant interaction term indicated that scale and interscale regions differed in EINS between treatments, and these data are shown in Table 6. Specifically, as compared to the resting condition, EINS in the scale region increased by 12% in the moderately stretched condition but only by 3% in the highly stretched condition. Thus, in the scale region EINS was significantly lower in the highly stretched condition than in the moderately stretched condition. In the interscale region, EINS increased by 17% between the unstretched and moderately stretched condition and by an additional 33% between the moderately stretched and highly stretched condition (Table 6). This suggests that during high levels of lower jaw extension, strain imposed on the whole lower jaw was translated to the cells of the interscale epidermis to a higher degree than the cells of scale epidermis.

The morphological changes in the epidermis varied considerably with each treatment. Micrographs of resting (Figs. 7 and 8), moderately stretched (Fig. 9) and highly stretched (Fig. 10) conditions illustrated the differences between the scale and interscale regions in response to each treatment. The scale epidermis changed relatively little as compared to interscale regions, and the most drastic effect was the bending or straightening of the curved free margins of scales. The cells of the stratum germinativum in the scale region retained a columnar-cuboidal morphology in all three conditions. SEM micrographs of the surface resting and highly stretched epidermis showed that the superficial surface of the scale epidermis remained intact and relatively smooth across these two treatments (Figs. 7C and 10B).

Table 5. Scale–scale interactions differing significantly ($P < 0.05$) across three treatment groups.

| | Treatment | |
|---|---|---|
| | Mod | High |
| Treatment | | |
| Rest | **L1L1**, **AA**, **AL4**, **PP**, PL5, PL6 | ML1, **L1L1**, L1A, **AA**, **AL4**, **PP**, PL5, PL6 |
| Mod | | **L1L1**, **AA**, **AL4**, **PP** |

Abbreviations are defined in Figure 3. Distances between scales (4) that differed across all three treatments are in bold.

Table 6. Comparison of scale and interscale epidermal (stratum germinativum) cell internuclear spacing (in μm) among three treatments.

| | Treatment | | |
|---|---|---|---|
| | Rest | Mod | High |
| Region | | | |
| $Scale_{n=390}$ | 2.95 ± 0.560[a] | 3.31 ± 0.540 | 3.05 ± 0.60[a] |
| $Interscale_{n=362}$ | 3.15 ± 0.770 | 3.67 ± 0.882 | 4.91 ± 1.30 |

[a]Values that are not significantly different at $\alpha = 0.05$. $n$ = number of cell pairs sampled. Abbreviations as in Table 4.

Table 7. Differences in average interscale fold amplitude (in μm) among three treatment groups.

| | Treatment | | |
|---|---|---|---|
| | Rest | Mod | High |
| Region | | | |
| $AA_{n=30}$ | 15.9 ± 9.11 | 9.80 ± 6.13 | 6.34 ± 4.09 |
| $AL_{n=30}$ | 11.1 ± 4.44 | 7.67 ± 3.78 | 10.53 ± 7.65 |
| $Total_{n=60}$ | **13.5 ± 7.51** | **8.76 ± 5.20** | **4.70 ± 3.47** |

Values shown are from two interscale regions sampled (AA and AL). Abbreviations defined in text. $n$ = number of observations.

The morphology of the interscale epidermis underwent the most drastic change between treatments. The cuboidal cell shape and the characteristic bumpy nature of the superficial layers seen in the resting condition were retained in the moderately stretched condition (Figs. 8A, 8B, and 9B), and changes occurring in the moderately stretched condition were primarily associated with the unfolding of major skin folds (Figs. 8A–F and 9B). However, in the highly stretched condition, the major epidermal folds continued to flatten, and though the bumpy appearance of the superficial surface was maintained (Figs. 10C, 10E) the visible cellular layers appeared to flatten (Figs. 10C, 10F). Thus, as EINS increased, there was a marked change in epidermal cell morphology: cells that were cuboidal-round in appearance in the resting and moderately stretched conditions (Figs. 8B and 9B) took on flattened ovoid shapes when the epidermis was highly stretched (Fig. 10C).

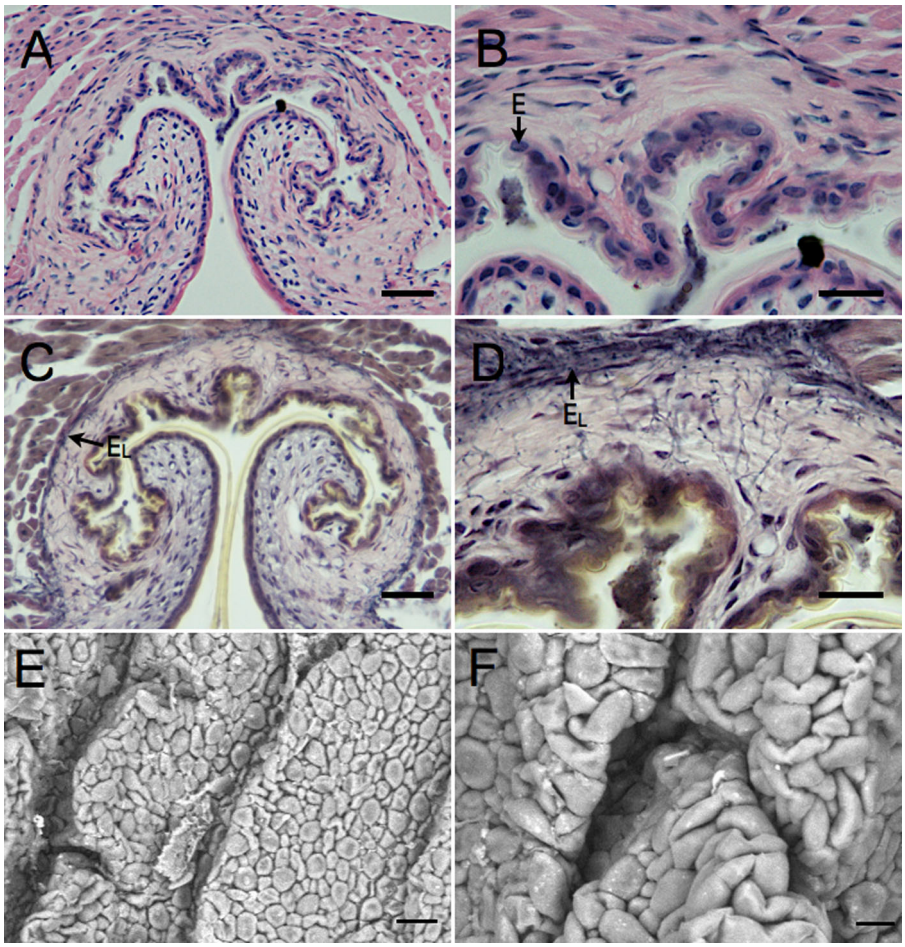


Figure 8. Cross-section of resting interscale skin between the anterior chin shields. (A) H&E, scale bar = 20 μm. (B) H&E, scale bar = 10 μm. E, epidermal stratum germinativum cell nucleus. (C) Elastin stain, scale bar = 20 μm. $E_L$, elastic lamina of the dermis. (D) Elastin stain, scale bar = 10μm. $E_L$ as in panel (C). (E) SEM image of outer interscale surface. Scale bar = 20 μm. (F) SEM image of outer interscale surface. Scale bar = 10 μm.

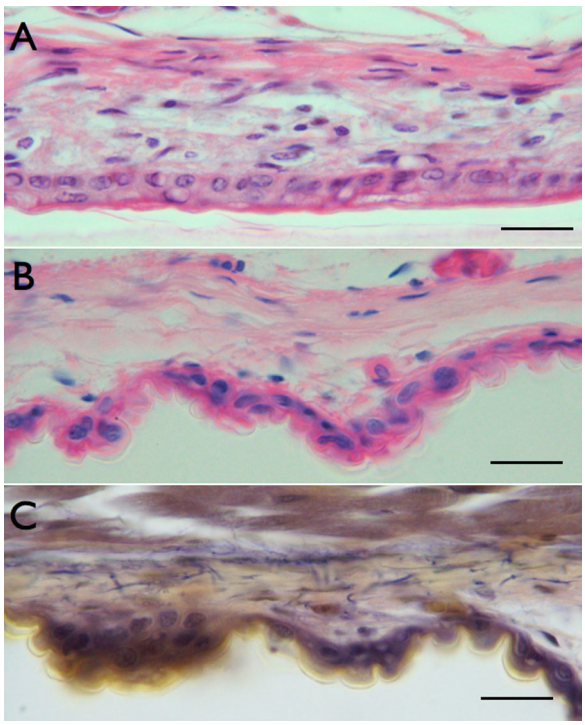


Figure 9. Cross-sections of scale and interscale regions of a moderately stretched specimen. (A) Scale region, H&E stain. (B) Interscale region, H&E stain. (C) Interscale region, elastin stain. In this condition elastin fibers (black) are still oriented in multiple planes. However, many are extending transversely in the plane of stretch. Scale bars = 10 μm.

### Histology: Dermal Changes

As noted previously by Pockrandt ('37), the dermis of snakes was composed of two primary layers distinguished both by collagen size and distribution as well as elastin content. The superficial dermis was composed of thin, orthogonally arranged, loosely packed collagen fibers with mesenchymal fibroblasts dominating cellular content. These regions were more highly vascularized and innervated than the deeper layers, and elastin content was relatively low. The deep dermis was composed of thicker, transversely oriented, parallel/braided bundles of collagen. Elastin was more abundant in the deep dermis and its density increased with depth terminating eventually into a thick, transverse band (elastic lamina) composed of (visually) more than 50% elastin in composition. In the region below the free margin of the scale (i.e., *inner scale surface + hinge*) collagen fibers coursed in multiple directions and appeared to be arranged more loosely than in the deep dermis of the scale base and in the interscale dermis. In resting skin, the interscale region was devoid of superficial dermis except within portions of major folds that had a loose arrangement of collagen and a higher density of blood vessels. The elastin in the interscale region formed a deep elastic lamina from which superficial fibers radiate, and this lamina was continuous with the lamina in the deep dermis of the scale regions.

The overall thickness of snake skin was difficult to measure because (1) it was divided into scale and interscale regions, each varying in thickness (Fig. 7A) and (2) because the interscale regions were highly folded in the resting condition (Figs. 8A–F). In regard to the latter, thickness, and therefore cross-sectional area, of the region depended on the (1) amplitude of the folds at a particular stretched condition and (2) the degree to which the dermis continued to stretch once the folds flattened.

We first compared average fold amplitude (FA) from two scale pairs (AA and AL4) across the three treatment groups using a two-way factorial ANOVA. Values for average FA for each scale pair and across three treatments are shown in Table 7. Our ANOVA indicated that treatment groups ($F_{(1,188)} = 41.97$, $P < 0.01$) and regions ($F_{(1,188)} = 19.736$, $P < 0.01$) differed significantly in FA. However, there was no significant interaction between treatment and region (AA vs. AL4) sampled ($F_{(2,188)} = 1.014$, $P = 0.365$), and, therefore, interscale regions, though different in absolute FA, responded to stretch by similar decreases in FA. Post hoc tests revealed FA decreased from the resting condition by 35% in the moderately stretched condition ($P < 0.01$) and by 65% in the highly stretched condition ($P < 0.01$). FA was 46% lower in the highly stretched condition than it was in the moderately stretched condition ($P < 0.01$). Thus, as our epidermal and dermal records indicate, and has been assumed for over a century (Ficalbi, 1888), the extension of snake skin primarily involves the unfolding of the interscale region.

Because the superficial dermis varied in thickness and was non-uniform, we measured the thickness only of the deep dermis across three treatment groups, and compared treatments using a one-way ANOVA. Values of dermal thicknesses among three treatments are summarized in Table 8. Our one-way ANOVA results showed that the average thickness of the deep dermis varied across treatment groups ($F_{(2,183)} = 8.09$, $P < 0.01$). Post hoc analyses indicated that the average deep dermal thickness in the moderately stretched condition was significantly less than the resting condition ($P < 0.05$). However, the resting condition and highly stretched condition did not differ significantly ($P = 0.11$) and the highly stretched condition was significantly thicker ($P < 0.01$) than the moderately stretched condition.

We used average internuclear spacing of fibroblasts in the dermis (DINS) to determine the degree to which this part of the skin changes with stretch treatment. We first sought to determine whether and how the dermal strata in the scale regions responded to stretch. Therefore, we used a two-way factorial ANOVA and tested the interaction between treatment and dermal strata. Our ANOVA showed that average DINS differed between treatment groups ($F_{(2,114)} = 38.05$, $P < 0.001$) and indicated a significant interaction between treatment and dermal stratum

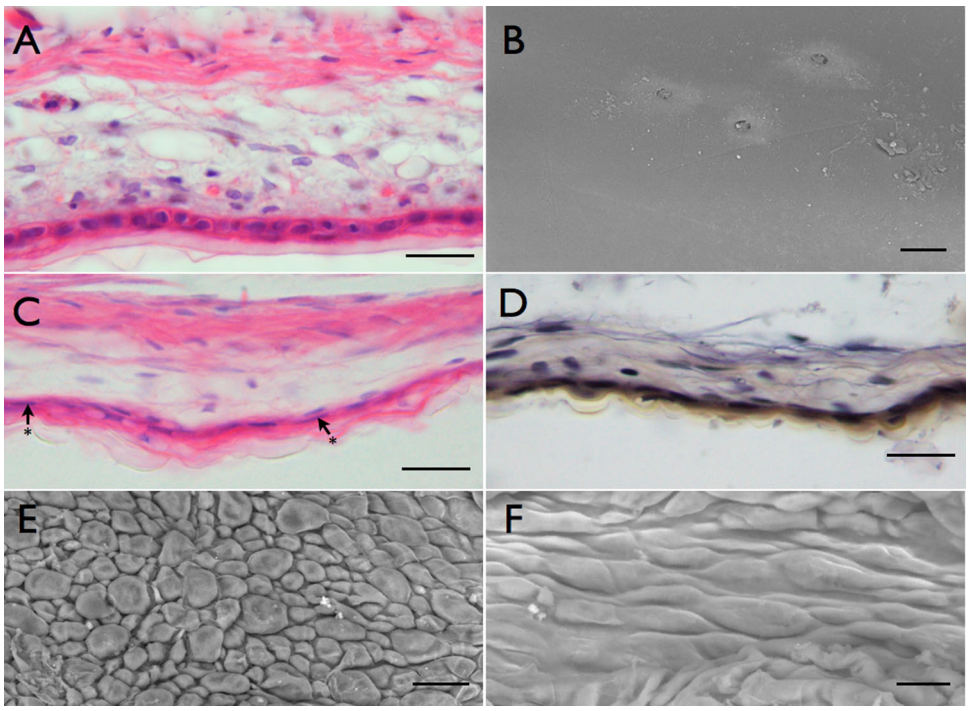


Figure 10. Cross-sections of scale and interscale regions of highly stretched skin. (A) Scale region, H&E stain, scale bar = 10 μm. (B) Scanning electron micrograph of scale region showing a lack of change in the outer scale surface. Scale bar = 60 μm. (C) Interscale region, H&E stain, scale bar = 10 μm. Arrows indicate cell nuclei in the epidermis. Cells become flattened as the epidermis is stretched. (D) Interscale region, elastin stain, scale bar = 10 μm. Elastin fibers (black) thin and more laterally oriented as they become stretched further. The elastic lamina is present in this section but is partly out of the focus so that supralaminal fibers can be seen. These superficial fibers extend laterally spanning a region folded in the resting state. (E) SEM image of interscale epidermis showing a region that has been unfolded but apparently not stretched because cells are still clustered together and form the minor folds of epidermis. Scale bar = 20 μm. (F) SEM image of interscale epidermis showing a region that is both completely unfolded and highly stretched. Keratin associated cell surface shows significant deformation in plane of stretch. Scale bar = 10μm.

($F_{(2,1144)} = 12.42$, $P < 0.01$; see Table 9). In the superficial dermis, DINS increased by only 3% in the moderately stretched condition and by only 16% in the highly stretched condition. Furthermore, DINS in the highly stretched condition was only 12% higher than the moderately stretched condition. In contrast, DINS in the deep dermis increased by 35% in the moderately stretched treatment and by 57% in the highly stretched condition. The deep dermis therefore exhibited a much more marked response to stretch than the superficial dermis.

Table 8. Differences in average deep dermal thickness (in μm) and fibroblast internuclear spacing (DINS, in μm) among three treatment groups.

| | Treatment | | |
|---|---|---|---|
| | Rest | Mod | High |
| Thickness $_{n=186}$ | 11.19 ± 4.62 | 9.75 ± 2.78 | 12.37 ± 4.22 |
| DINS$_{n=761}$ | 7.29 ± 3.46 | 9.51 ± 4.36 | 10.45 ± 4.02 |

Samples collected from both scale and interscale regions. DINS was significantly different across all treatments at α = 0.05. For Thickness, lines connect group means that were not significantly different at α = 0.05. *n* = number of samples. Abbreviations as in Table 4.

Table 9. Dermal effects at the level of the scale: Comparison of fibroblast internuclear spacing (in μm) in superficial and deep layers of scale dermis across three treatment groups.

| | Treatment | | |
|---|---|---|---|
| | Rest | Mod | High |
| Layer | | | |
| Superficial$_{n=759}$ | 7.18 ± 2.90 | 7.44 ± 2.82 | 8.35 ± 3.15 |
| Deep$_{n=391}$ | 6.88 ± 3.89 | 9.29 ± 4.37 | 10.81 ± 4.50 |

*n* = number of fibroblast pairs measured. Abbreviations as in Table 4.

Our comparison of DINS of interscale dermis revealed a significant difference across treatment groups ($F_{(2,758)} = 34.01$, $P < 0.001$). Post hoc analyses indicated that DINS increased significantly by 30% between the resting and moderately stretched condition ($P < 0.01$) and by 43% between the resting and highly stretched conditions. Similarly, DINS increased by 10% between the moderately stretched and highly stretched conditions ($P < 0.01$). Therefore, though we did not directly compare the deep dermis of scale region to the dermis of interscale region, the two responded to extension in similar ways.

### Elastin

Pockrandt ('37) first described the distribution of elastin in the deep dermis of snake body skin. While some studies indicate that elastin in mammal skin makes up a mere 4% by mass of the total dermal content (Gibson and Kenedi, '70), its composition throughout the depth of the dermis is variable. In the resting condition of snake skin, the deepest layers of the dermis contained abundant elastin. Together these fibers formed a thick dermal elastic lamina from which thinner fibers radiated superficially through the deep dermis and were associated closely with collagen in the extracellular matrix and basement membrane of the epidermis (Figs. 8C, 8D). The elastic layer coursed transversely through the deep dermis of the scale as well as the interscale regions, and elastic fibers extended from the elastic lamina superficially to the hinge region of the scale (inner scale surface below free margin) and the base of folds in the dermis. In the scale region superficial excursions of elastin into the superficial dermis were relatively rare, and most of the elastin was closely associated with the parallel collagen fibers of the deep dermis.

The elastin fibers radiating out of the elastic lamina were anchored presumably to the basal lamina (basement membrane) of the interscale epidermis at particular regions (i.e., the base of folds). In the moderately stretched condition (Fig. 9C), the dermal folds of interscale skin began to unfold and the elastic lamina began to stretch in the transverse plane. Meanwhile, the fibers radiating from this layer began to stretch as the anchoring sites on the elastic lamina moved further away from one another. In the highly stretched condition, the folds flattened, and superficial fibers became thinner and oriented transversely (Fig. 10D). In this highly extended state, the elastic lamina and the fibers that coursed from it were presumably at lowest entropy. Therefore, when the load was released, the elastic lamina and the radiating fibers should have both acted to return scales to their resting position and return folds of hinge and interscale epidermis to their resting condition.

### Nerve Supply

The scales of the lower jaw are innervated by the mandibular branch of the trigeminal nerve ($V_3$, Auen and Langebartel, '77), and scales we examined were innervated by at least three divisions of this nerve. The posterior chin shields were innervated by a small branch that exited a foramen on the medial surface of the angular bone posteriorly, as well as a branch that exited the anterior mandibular foramen. The anterior chin shields were innervated only from the latter branch, which was branched extensively at the level of the anterior chin shield and coursed anteriorly to terminate finally in the first lower labial scales. The first lower labials, in addition to being innervated by this branch, were innervated also from a branch that supplies all other labials. This latter branch exited the mental foramen on the lateral surface of the dentary and sent fibers anteriorly into the mental scale as well as posteriorly to supply the infralabials (Fig. 11A).

Very few of these nerve fibers were highly convoluted in the resting condition but most major nerve branches were arranged longitudinally. One peculiarity of nerve distribution was that at least one major branch innervated several inextensible scales and crossed several extensible interscale regions as it coursed anteriorly. This arrangement presented obvious problems with scale innervation that were evident when the lower jaw was stretched (Fig. 11B). Specifically, nerves seem to be anchored to the inextensible portions of skin (scales) but reorientation of larger nerve branches, from longitudinal to transverse, occurred when the lower jaw was highly extended.

Examination of serial sections through the junction between the anterior chin shield and the adjacent first lower labial scale showed that regions of the nerve between adjacent scales (i.e., crossing the interscale region) coursed deep to the dermis. As seen in Figure 11, $V_3$ coursed just below the dermis of the scale, and sent fibers superficially to the anterior chin shield, crossing the bilayered scale dermis at certain points along this scale. The nerve coursed immediately deep to the dermis as it crossed the interscale region toward the first lower labial scale, eventually crossing the dermis into the base of the first labial scale, which it entered. Therefore, the nerve appeared to be "anchored" to the scale at points close to the scale sense organs from which it receives input.

In the stretched dermis (Fig. 11B), there was gross reorientation of nerve fibers from longitudinal to transverse, but exactly whether and how peripheral branches of nerves moved relative to one another was difficult to determine. Based on the relationship of the nerves to the scales (Fig. 12), it is likely that reorientation occurred without a great deal of extension.

## DISCUSSION

Previous analyses of the performance of the feeding apparatus in watersnakes have used measures of skeletal or external head features that are easy to record and correlate to gape size (Queral-Regil and King, '98; Vincent et al., 2006a,b, 2007; Herrel et al., 2008; Hampton, 2010, 2011). Although differences in gape size among snake species correlate to lengths of skeletal elements such as the quadrate and mandible (Hampton, 2011), gape size in snakes is also dependent on extensibility of soft tissues connecting the tips of the dentaries (Hampton and

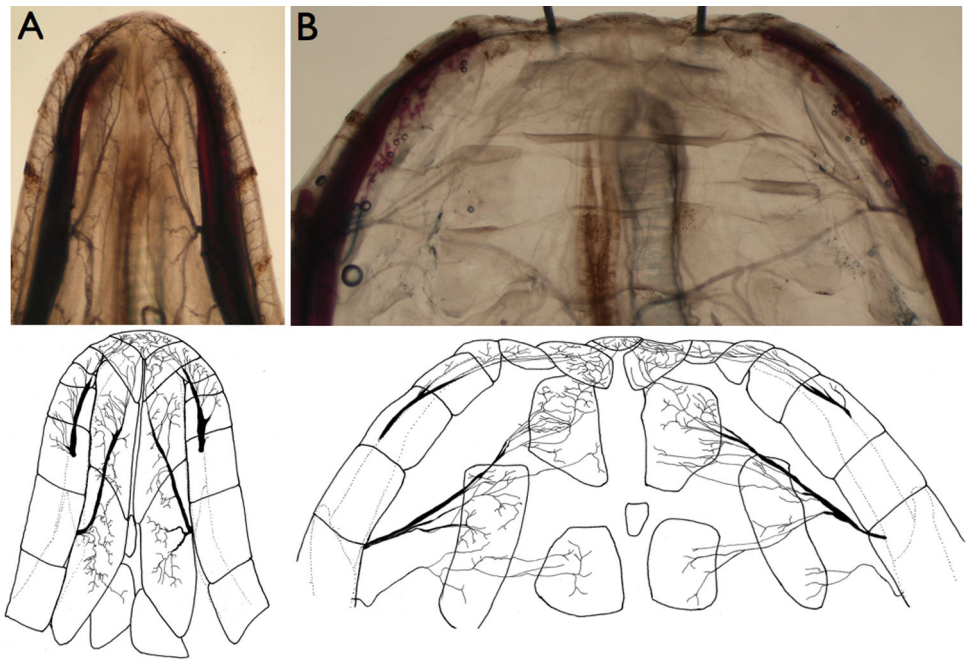


Figure 11. Patterns of scale innervation. (A) Resting. (B) Stretched. In each, the upper picture is a cleared and stained specimen and the lower is an ink tracing of nerves and scale outlines. Dotted lines represent the mandibles.

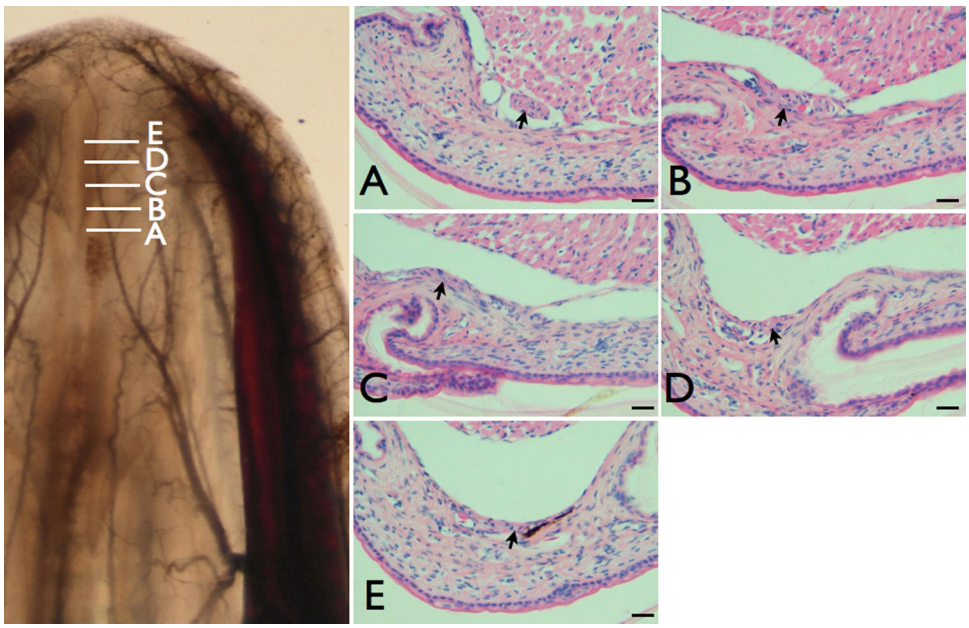


Figure 12. Serial cross-sections (A–E, posterior to anterior) through the junction between anterior chin shield and first labial scales showing course and entry of nerve (arrow) and adjacent blood vessel into base of first labial scale. Scale bars = 10 μm.

Moon, 2013). Field experiments have shown that gape cross-sectional area, when calculated from head width and jaw length alone, underestimates observed prey cross-sectional area, and this suggests an important role for extensible intermandibular soft tissues in determining maximum gape size (King, 2002). Although the latter has been generally accepted, intermandibular distance has been empirically measured in live snakes in only a single study (Vincent et al., 2006b) and in a single study of dead, frozen/thawed snake head and gape measurements (Hampton and Moon, 2013). The results showed that intermandibular distance was significantly positively correlated to gape size and prey width, but unfortunately no clear explanation was provided of how intermandibular separation occurred. Finally, studies of snake feeding performance that have used ingestion rate as a measure have generally used prey well below the maximum size the snake could swallow. As a result, we know little about the real gape potential of most snakes.

During feeding (intraoral prey transport: Cundall and Greene, 2000) the mandibles of watersnakes separated slightly beyond 7× their distance at rest, and the process took more than 20 min in some cases. Therefore, ingesting large prey involves extending tissues over relatively long periods of time. Our mechanical tests partially corroborate this relationship: intermittent increases in strain allowed the mandibles to separate to 10× their resting distance without failure. Few anatomical structures in vertebrates have this capability (Brainerd, '94; Wainwright et al., '76; Vogel, 2003). We analyzed some of the structural results of extension in the skin to refine hypotheses of the mechanism of tissue extensibility. Recent studies of snake skin have dealt with its mechanical properties in the context of locomotion (Jayne, '88; Berthé et al., 2009; Klein et al., 2010) and macrostomy (Rivera et al., 2005). Even though it has long been noted that snake interscale skin stretches more than scale regions, to date, only two studies (Pockrandt, '37; Savitzky et al., 2004) have given serious attention to the anatomical basis of the ability of skin to stretch. Savitzky et al. (2004) showed that there was a correlation between dorsal scale row arrangement and macrostomy, or the ability of the skin to stretch circumferentially. They suggested that arrangements of body scales and interscale regions correlated with the ability to stretch in the circumferential axis. Thus, the extensibility of skin as a whole was dependent on the arrangement of scale rows relative to the long axis of the body. Savitzky et al. (2004) also suggested that the ability of the skin to recover from a stretched condition was aided by elastin networks that spanned the interscale region. Our histological data shows that the ability of folded interscale skin to unfold during stretch and refold when relaxed rests in the structure, composition and behavior of the deep dermis (*stratum compactum*).

### Arrangement of Nerves

The degree of extension of nerves is limited by the mechanical properties of the perineural sheath as well as the physiological properties of the cell bodies and neurites. The effects of stretching on conduction velocity have been documented relatively well for over 100 years. Recent studies indicate that the physiological effects of low levels of extension are reversible, while high levels of extension (greater than 20%) exhibit irreversible, pathologic effects (Kwan et al., '92; Li and Shi, 2007; Galbraith et al., '93; Tanoue et al., '96). High levels of strain affect both the perineural sheath in addition to demyelinating the axon (Rydevik et al., '90; Kubota et al., 2011). Physiological and morphological data support the general conclusion that most nerves are not well suited for relatively high levels of extension. The perineural sheath lacks the (1) bi-directional orientation of collagen fibers and (2) relatively abundant elastin found in highly extensible connective tissues. The arrangement and mechanical properties of collagen (Fratzl, 2008) comprising much of the perineural sheath should therefore dictate the physiological limits to which nerves can be stretched. Two noteworthy modifications seem to permit nerve extension (1) orienting nerves along the axis that is perpendicular to the plane of stretch and/or (2) convoluting the nerve (with subsequent pleating of the perineural sheath). A high degree of convolution was not detected by the methods we used for snakes, but we did find that the gross orientation of branches of the trigeminal (V3) nerve that innervates scales tended to be arranged longitudinally. This orientation permits lateral/circumferential extension while imposing minimal stress on the nerve branches themselves. Further histological work on the perineural sheath is required to determine the degree of crimping and how it is affected by degrees of extension used in our study. While we also showed that nerve branches are "anchored" to scales via the deep dermis, it was difficult to determine whether and how these anchoring sites themselves changed at high levels of extension. Finally, it remains to be seen how much strain was imposed on these nerves when a high degree of intermandibular separation occurred and what the physiological consequences of this were.

### A Model of Snake Skin Extensibility

The resting condition of skin is distinguished from the stretched conditions by folding of the interscale skin (Fig. 13A). Dermal ridges, covered by thin interscale epidermis, produce the major folds. At rest the cells of the interscale epidermis take on a variety of shapes, but the predominant shape of the living cells (i.e., the stratum germinativum and the *cellules à mamelon*) is cuboidal. Due to the extensive folding the cells are packed closely together and, in combination with the bizarre shapes of the *cellules à mamelon*, form minor folds in the surface. The collagen fibers of the deep dermis are thick and are parallel or braided in the interscale and scale regions, and parallel or woven and orthogonal in the hinge regions. The deepest layer of the dermis forms an elastic lamina from which elastin fibers radiate transversely, orthogonally and superficially at the base of the major folds.

The moderately stretched condition (Fig. 13B) is characterized primarily by an unfolding of the major folds of interscale skin. As

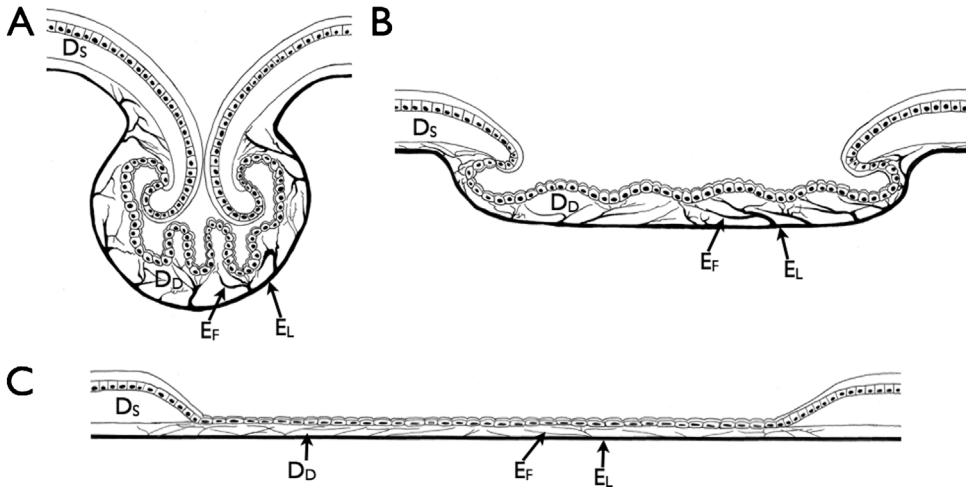


Figure 13. Model of skin stretching. (A) Resting. (B) Moderately stretched. (C) Highly stretched. For simplicity, the outer strata and keratinized layers of the epidermis are not distinguished and appear as a single layer outside of the stratum germinativum. $E_L$, elastic lamina; $E_F$, elastin fiber; $D_S$, superficial dermis; $D_D$, deep dermis.

the region unfolds, cells in the epidermis become less packed, and this is accompanied by a slight increase in the distance between nuclei. However, cell shape does not change drastically and the minor folds of the surface are preserved. The dermis responds to unfolding in a slightly more dramatic way—the collagen fibers tend to be reoriented in the plane of extension and the elastin fibers begin to stretch as the basement membrane of the epidermis and the elastic lamina of the dermis extend. Fibroblasts in the dermis are spaced farther apart, indicating that strains are occurring in the extracellular matrix at the histological, and possibly cellular, levels. The moderately stretched condition can therefore be described as an unfolding of the epidermis and a flattening/straightening of the dermis.

The highly stretched condition (Fig. 13C) is characterized as a further unfolding and (at least in some cases) stretching of the interscale epidermis and dermis. The major folds disappear and many of the minor folds decrease in amplitude. The latter is associated with changes in cell shape as the cells of the interscale epidermis become flattened. The distance between nuclei of cells in this layer also increases which suggests that deformations/strains are occurring at the cellular level. The dermis responds to continued extension by stretching. Once the interscale folds flatten, most collagen fibers, many of which are located in folded regions, become oriented in the plane of stretch and subsequently stretch minimally as added load is applied. The thickness of the deep dermis increased in this condition. Although it is possible that this was an artifact of preparation, it is also possible that extension in the transverse/circumferential axis imposed compression in the longitudinal axis resulting in an overall increase in thickness. The gross affect of compression on scales deformation was evident in examining stretched specimens and during in vivo testing (see Figs. 3 and 6), and the same effect was likely for interscale skin, though it was not visualized clearly at the gross level. Elastin fibers continue to lengthen and thin (to the point where some are difficult to identify with the light microscope), but seem to still maintain their association with the basement membrane of the epidermis and the elastic lamina of the dermis.

How, then, does the skin return to its resting folded condition? Our histological data suggest that passive elastic recoil accounts for much of the refolding of the interscale epidermis. In the unstretched condition, the endings of elastin fibers appear to be associated with the basement membrane of the epidermis preferentially in the "valleys" between folds of the skin and occasionally with adjacent and opposite walls of folds (Fig. 14A). Fibers either course directly to the elastic lamina of the dermis or

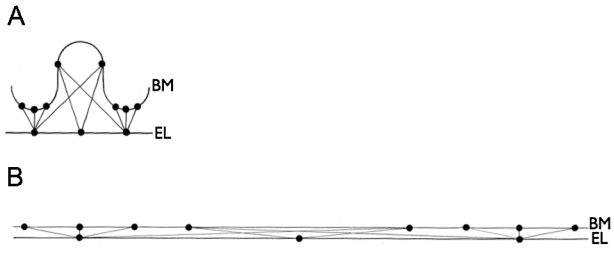


Figure 14. Model of unfolding and refolding mechanism based on histological data. (A) Resting condition. (B) Stretched condition. Elastin fibers extend from the elastic lamina (EL) of the deep dermis and are presumably anchored to points (•) along the basement membrane (BM) of the epidermis at the dermo-epidermal boundary.

converge with other fibers at trunks, which then meet the elastic lamina, but in either case, elastin fibers appear to extend from the epidermal basement membrane to the dermal elastic lamina (Fig. 14B). When the folded regions are stretched, the distance between these presumed elastin attachment sites increases. Refolding of the interscale skin occurs when the load is released and elastin recoils. Attachment sites on the elastic lamina come closer together bringing the dermis of the "valleys" closer together. At the same time the depth of the "valleys" is recovered via the recoil of elastin fibers, which extend between the basement membrane and the elastic lamina.

The deformation of the dermis is dominated by reorganization of the extracellular matrix and by extension of the elastin that composes a large portion of its deep layer. Under a relatively high strain rate, the reorientation of collagen fibers would occur, but tension would rise more quickly as collagen fibers would remain cross-linked and fairly rigid. Under slow strain rates, which may reduce cross-linking, fibers presumably reorient and slide relative to one another increasing the potential for irreversible creep (Craig et al., '87). Return from this state therefore requires the recovery of the stretched elastin, which remains anchored at the basement membrane and the elastic lamina.

At higher strain rates, it is unlikely that the epidermis would do more than unfold since tension would rise primarily in the underlying dermis before strain was imposed on the cells of the epidermis. However, under low strain rates (as used in our study and during feeding by the snakes), the folds flatten and cells of the epidermis stretch slowly and become flattened. In order for cells to remain in their location during periods of stretch, membrane proteins on their basolateral surfaces would have to rearrange to allow the basal surfaces to extend with the basement membrane and the lateral surface to reduce its attachment to neighboring cells as cell cross-sectional area decreases. The decrease in cell cross-sectional area occurs in all superficial cell layers. At high levels of extension, the soft alpha keratin of the superficial layers unfolds and subsequently refolds when the load is reduced. Return from the highly extended state would require further reorganization at the basolateral surfaces of cells—probably until the resting state is fully recovered. The types of changes seen in the epidermis are not well documented in the literature and require further investigation using ultrastructural techniques.

The architecture of squamate skin contains the structural potential to evolve from a movable armor sufficient for locomotion (e.g., lizards and amphisbaenians) to an extensible armor well suited for macrostomy (snakes). This unique integument is not the only feature limiting intermandibular extensibility, but it is integrated with the network of deeper tissues linking the mandibles and thus plays a critical role. Furthermore, its response to mechanical stress (stretching) exhibits features that may be shared among other intermandibular soft tissues. Whether other highly extensible vertebrate tissues share the passive intra- and extracellular elastic mechanisms that have evolved in snakes to recover their resting state remains to be seen.

## ACKNOWLEDGMENTS

We thank Richard Vinci for his assistance with mechanical testing and Bruce Hargreaves and Joseph Seem for their assistance with the scanning electron microscope. Critical reviews of earlier drafts of this manuscript were provided by Alan Savitzky, Nathan Kley, Matthias Falk, Lynne Cassimeris, and Brooke Hopkins Dubansky. This study was funded in part by an E.E. Williams Graduate Research Grant from the Herpetologists' League to MC.

## LITERATURE CITED

Alibardi L. 2002. Ultrastructure of the embryonic snake skin and putative role of histidine in the differentiation of the shedding complex. J Morphol 251:149–168.

Alibardi L, Thompson MB. 1999. Epidermal differentiation in the developing scales of embryos of the Australian scincid lizard *Lampropholis guichenoti*. J Morphol 241:139–152.

Alibardi L, Thompson MB. 2003. Epidermal differentiation during ontogeny and after hatching in the snake *Liasis fuscus* (Pythonidae, Serpentes, Reptilia), with emphasis on the formation of the shedding complex. J Morphol 256:29–41.

Arnold SJ. 1983. Morphology, performance, and fitness. Am Zool 23:347–361.

Auen EL, Langebartel DA. 1977. The cranial nerves of the colubrid snakes *Elaphe* and *Thamnophis*. J Morphol 154:205–222.

Baden HP, Roth SI, Bonar LC. 1966. Fibrous proteins of snake scales. Nature 212:498.

Banerjee TK, Mittal AK. 1978. Histochemistry of the epidermis of the chequered water snake Natrix piscator (Colubridae, Squamata). J Zool 185:415–435.

Banerjee TK, Mittal AK. 1980. Histochemistry of snake epidermis. In: Spearman RIC, Riley PA, editors. The skin of vertebrates. London: Academic Press. p 23–32.

Berthé R, Westho VG, Bleckmann H, Gorb S. 2009. Surface structure and frictional properties of the skin of the Amazon tree boa *Corallus hortulanus* (Squamata, Boidae). J Comp Physiol A 195:311–318.

Brainerd EL. 1994. Pufferfish inflation: functional morphology of postcranial structures in *Diodon holocanthus*. J Morphol 220: 243–261.

Brusca RC, Brusca GJ. 2003. Invertebrates. 2nd edition. Sunderland, MA: Sinauer.

Chiasson R, Lowe C. 1989. Ultrastructural scale patterns in *Nerodia* and *Thamnophis*. J Herpetol 23:109–118.

Chiasson R, Bentley DL, Lowe C. 1989. Scale morphology in *Agkistrodon* and closely related crotaline genera. Herpetologica 45:430–438.

Churukian J, Schenk E. 1976. Iron gallein elastic method—a substitute for Verhoeff's elastic tissue stain. Stain Technol 51: 213–217.

Craig A, Eikenberry E, Parry D. 1987. Ultrastructural organization of skin: classification on the basis of mechanical role. Connect Tissue Res 16:213–223.

Cundall D, Deufel A. 2006. Influence of the venom delivery system on intraoral prey transport in snakes. Zool Anz 245:193–210.

Cundall D, Greene HW. 2000. Feeding in snakes. In: Schwenk K, editor. Feeding: form, function and evolution in tetrapod vertebrates. San Diego: Academic Press. p 293–333.

Debelle L, Tamburro AM. 1999. Elastin: molecular description and function. Int J Biochem Cell Biol 31:261–272.

Ficalbi E. 1888. Ricerche istologiche sul tegumento dei serpenti. Atti Soc Toscana Sci Nat, Pisa, 9, fasc. 1 (reviewed, in French, in Arch Ital Biol 10: 401–418.)

Fratzl P, editor. 2008. Collagen: structure and mechanics. New York: Springer Science Business Media.

Galbraith JA, Thibault LE, Matteson DR. 1993. Mechanical and electrical responses of the squid giant axon to simple elongation. J Biomech Eng 115:13–22.

Gans C. 1961. The feeding mechanism of snakes and its possible evolution. Am Zool 1:217–227.

Gans C. 1974. Biomechanics: an approach to vertebrate biology. Philadelphia: J.B. Lippincott Company.

Gibson T, Kenedi RM. 1970. The structural components of the dermis and their mechanical characteristics. In: Montagna W, Bentley JP, Dobson, RL editors. Advances in biology of skin, vol. 10: the dermis. New York: Appleton-Century-Crofts. p 19–38.

Gower D. 2003. Scale microornamentation of uropeltid snakes. J Morphol 258:249–268.

Hampton PM. 2010. Morphology, behavior, and physiology of feeding in snakes [doctoral dissertation]. Lafayette, IN: University of Louisiana at Lafayette.

Hampton PM. 2011. Comparison of cranial form and function in association with diet in natricine snakes. J Morphol 272:1435–1443.

Hampton PM, Moon BR. 2013. Gape size, its morphological basis, and the validity of gape indices in western diamond-backed rattlesnakes (*Crotalus atrox*). J Morphol 274:194–202.

Herrel A, Vincent SE, Alfaro ME, Van Wassenbergh S, Vanhooydonck B, Irschick DJ. 2008. Morphological convergence as a consequence of extreme functional demands: examples from the feeding system of natricine snakes. J Evol Biol 21:1438–1448.

Hoge A, Santos S. 1953. Submicroscopic structure of "stratum corneum" of snakes. Science 118:410–411.

Humason GL. 1979. Animal tissue techniques. 4th edition. San Francisco: WH Freeman.

Irish FJ, Williams EE, Seling E. 1988. Scanning electron microscopy of changes in epidermal structure occurring during the shedding cycle in squamate reptiles. J Morphol 197:105–126.

Jackson MK, Reno HW. 1975. Comparative skin structure of some fossorial and subfossorial Leptotyphlopid and Colubrid Snakes. Herpetologica 31:350–359.

Jackson MK, Sharawy M. 1980. Scanning electron microscopy and distribution of specialized mechanoreceptors in the Texas rat snake *Elaphe obsoleta lindheimeri* (Baird and Girard). J Morphol 163:59–67.

Jayne B. 1988. Mechanical behaviour of snake skin. J Zool Lond 214:12–140.

Joseph P, Mathew J, Thomas V. 2007. Scale morphology, arrangement and micro- ornamentation in *Xenochrophis piscator* (Schneider), *Naja naja* (Linn), and *Eryx johni* (Russell). Zoo's Print J 22:2909–2912.

Kardong KV. 2012. Vertebrates: comparative anatomy, function, evolution. 6th edition. New York: McGraw-Hill.

King RB. 2002. Predicted and observed maximum prey size–snake size allometry. Funct Ecol 16:766–772.

Klein M-CG, Deuschle JK, Gorb SN. 2010. Material properties of the skin of the Kenyan sand boa *Gongylophis colubrinus* (Squamata, Boidae). J Comp Physiol A 196:659–668.

Kley NJ. 2006. Morphology of the lower jaw and suspensorium in the Texas blindsnake, *Leptotyphlops dulcis* (Scolecophidia: Leptotyphlopidae). J Morphol 267:494–515.

Kubota S, Nishiura Y, Hara Y, Abe I, Ochiai N. 2011. Functional and morphological effects of indirect gradual elongation of peripheral nerve: electrophysiological and morphological changes at different elongation rates. Hand Surg 16:105–111.

Kwan, MK, Wall, EJ, Massie, J, Garfin, SR. 1992. Strain, stress and stretch of peripheral nerve. Rabbit experiments ex vivo and in vivo. Acta Orthop Scand 63:267–272.

Landmann L. 1986. Epidermis and dermis. In: Hahn J, Matoltsy A, Richards K, editors. Biology of the integument, vol. 2J. Berlin: Springer-Verlag.

Lange B. 1931. Integument der sauropsiden. In: Bolk L, Göppert E, Kallius E, Lubosch W, editors. Handbuch der vergleichenden Anatomie der Wirbeltiere, Band 1. Berlin: Urban & Schwarzenberg. p 375–448.

Li J, Shi R. 2007. Stretch-induced nerve conduction deficits in guinea pig ex vivo nerve. J Biomech 40:569–578.

Licht P, Bennet A. 1972. A scaleless snake: tests of the role of reptilian scales in water loss and heat transfer. Copeia 1972:702–707.

Lillywhite H, Maderson PFA. 1982. Skin structure and permability. In: Gans C, Pough FH, editors. Biology of the reptilia, vol. 12, physiology C: physiological ecology. London: Academic Press. p 397–442.

Maderson PFA. 1964. The skin of lizards and snakes. Br J Herpet 3: 151–154.

Maderson PFA. 1965a. Histological changes in the epidermis of snakes during the sloughing cycle. J Zool 146:98–113.

Maderson PFA. 1965b. The embryonic development of the squamate integument. Acta Zool 46:275–295.

Maderson PFA. 1985. Some developmental problems of the reptilian integument. In: Gans C, Billett F, Maderson PFA, editors. Biology

of the reptilia, vol. 14B. New York: John Wiley & Sons. p 525–598.

Mittal K, Singh N. 1987a. Scale epidermis of *Natrix piscator* during its sloughing cycle. Structural organization and protein histochemistry. J Zool Lond 213:545–568.

Mittal K, Singh N. 1987b. Hinge epidermis of *Natrix piscator* during its sloughing cycle. Structural organization and protein histochemistry. J Zool Lond 213:655–695.

Montagna W. 1962. The structure and function of skin. 2nd edition. New York: Academic Press.

Montagna W, Bentley JP, Dobson RL, editors. 1970. Advances in biology of skin, vol. 10: the dermis. New York: Appleton-Century-Crofts.

Moss M. 1972. The vertebrate dermis and the integumental skeleton. Am Zool 12:27–34.

Nishikawa KC. 1987. Staining amphibian peripheral nerves with Sudan Black B: progressive versus regressive methods. Copeia 1987:489–491.

Oxlund H, Manschot, J, Viidik A. 1988. The role of elastin in the mechanical properties of skin. J Biomech 21:213–218.

Partridge SM. 1970. The biological role of cutaneous elastin. In: Montagna W, Bently J, Dobson, R, editors. The dermis. New York: Meredith Corporation. p 69–86.

Pockrandt D. 1937. Beitrage zur Histologie der Schlangenhaut. Zool Jb Anat 62:275–322.

Price R. 1981. Analysis of the ecological and taxonomic correspondence of dorsal snake microdermatoglyphics [doctoral dissertation]. New York: New York University, 164p.

Price R. 1982. Dorsal scale microdermatoglyphics: ecological indicator or taxonomic tool. J Herpetol 16:294–306.

Queral-Regil A, King RB. 1998. Evidence for phenotypic plasticity in snake body size and head dimensions in response to amount and size of prey. Copeia 1998:423–429.

Rivera G, Savitzky AH, Hinkley JA. 2005. Mechanical properties of the integument of the common gartersnake, *Thamnophis sirtalis* (Serpentes: Colubridae). J Exp Biol 208:2913–2922.

Roth SI, Jones WA. 1967. The ultrastructure and enzymatic activity of the boa constrictor (*Constrictor constrictor*) skin during the resting phase. J Ultrastr Res 18:304–323.

Roth SI, Jones WA. 1970. The ultrastructure of epidermal maturation in the skin of the boa constrictor. (*Constrictor constrictor*). J Ultrastr Res 32:69–93.

Rydevik, BL, Kwan, MK, Myers, RR, et al. 1990. An ex vivo mechanical and histological study of acute stretching on rabbit tibial nerve. J Orthop Res 8:694–701.

Savitzky A, Townsend V Jr, Hutchinson D, Mori A. 2004. Dermal characteristics, scale row organization, and the origin of macrostomy in snakes. J Morphol 260:325.

Sherbrooke W, Scardino A. 2007. Functional morphology of scale hinges used to transport water: convergent drinking adaptations in desert lizards (*Moloch horridus* and *Phrynosoma cornutum*) Zoomorphology 126:89–102.

Swadźba E, Maślak R, Rupik W. 2009. Light and scanning microscopic studies of integument differentiation in the grass snake Natrix natrix L. (Lepidosauria, Serpentes) during embryogenesis. Acta Zool 90:30–41.

Swadźba E, Rupik W. 2010a. A comparative studies of scales and gastrosteges formation in grass snake *Natrix natrix* L.* (Lepidosauria, Serpentes) embryos. Acta Biol Crac Ser Bot 25:89.

Swadźba E, Rupik W. 2010b. Ultrastructural studies of epidermis keratinization in grass snake embryos *Natrix natrix* L. (Lepidosauria, Serpentes) during late embryogenesis. Zoology 113:339–360.

Tanoue M, Yamaga M, Ide J, Takagi K. 1996. Acute stretching of peripheral nerves inhibits retrograde axonal transport. J Hand Surg 21:358–363.

Vincent SE, Dang PD, Kley NJ, Herel A. 2006a. Morphological integration and adaptation in the snake feeding system: a comparative phylogenetic study. J Evol Biol 19:1545–1554.

Vincent SE, Moon BR, Shine R, Herrel A. 2006b. The functional meaning of "prey size" in water snakes (*Nerodia fasciata*, Colubridae). Oecologia 147:204–211.

Vincent SE, Moon BR, Herrel A, Kley N. 2007. Are ontogenetic shifts in diet linked to shifts in feeding mechanics? Scaling of the feeding apparatus in the banded watersnake, *Nerodia fasciata*. J Exp Biol 210:2057–2069.

Vogel, S. 2003. Comparative biomechanics: life's physical world. Princeton: Princeton University Press.

Wainwright SA, Biggs WD, Currey JD, Gosline JM. 1976. Mechanical design in organisms. Princeton: Princeton University Press.

Young BA. 1998a. The comparative morphology of the intermandibular connective tissues in snakes (Reptilia: Squamata). Zool Anz 237:59–84.

Young BA. 1998b. The comparative morphology of the mandibular midline raphe in snakes (Reptilia: Squamata). Zool Anz 237:217–241.